Heart Beat Detection Using Filter-Banks

Aaditya Prakash Kattekola
Electrical and Computer Engineering
University of California, Sanata Barbara, USA
aadityaprakash@ucsb.edu

***Abstract*—Electrocardiogram (ECG) signals are electrically measured heart pulses that give information about its condition. ECGs have been traditionally used as a non-invasive test to measure heart's electrical activity in order to detect any anomalies like artery blockage, irregular heartbeats etc. The implementation of ECG detection algorithms in wearables such as smartwatches, fitbits etc. is a testament to their efficacy in discerning ones health. This report presents a study of the ECG signals and a detection pipeline for finding heart beats using filter banks is also explored.**

I. Introduction

Electrocardiogram (ECG) signal processing is crucial for diagnosing and monitoring cardiovascular diseases (CVDs), which account for approximately 17.9 million deaths globally each year [1]. This non-invasive technique records the electrical activity of the heart, providing essential information for identifying conditions such as arrhythmias, ischemia, and other cardiac disorders. Traditional visual inspection of ECG signals has been transformed by advanced signal processing techniques, enhancing diagnostic accuracy and efficiency through automated detection of abnormalities [2] [3].

With the rise of wearable devices and telemedicine, ECG signal processing has expanded beyond hospitals, enabling real-time monitoring and personalized healthcare. These applications utilize robust filtering, feature extraction, and classification methods to ensure reliability under varying conditions [2].

This project explores the use of Filter Banks to detect heart beats from ECG signals. An overview of ECG signals is provided in Section II. In Section III, filter bank design fundamentals are highlighted. Section IV highlights the beat detection pipeline, describing the low frequency noise, the subbands of the signal and the feature used to detect the heart beat. The conclusion is presented in Section V along with contemporary research on ECG signal processing.

II. Electro-cardio-gram Signals

In this section, the cause of the ECG signal, it features and frequency characteristics are defined.

A. Electrical Activity of the Heart

The human heart has 4 chambers - 2 atria[1] at top and 2 ventricles at the bottom (Fig. 1 Left). When influenced by an electric provocation the heart muscles shrink, pushing blood into the body. This provocation propagates through the heart in the form of a depolarization wave of bioelectric energy. After depolarization, muscle cells come to resting phase known as the repolarization. Both the repolarization and depolarization are caused by the movement of ions which constitutes an electric current that also generates an electromagnetic (EM) field. It is possible to measure the electric potential across this EM field [4].

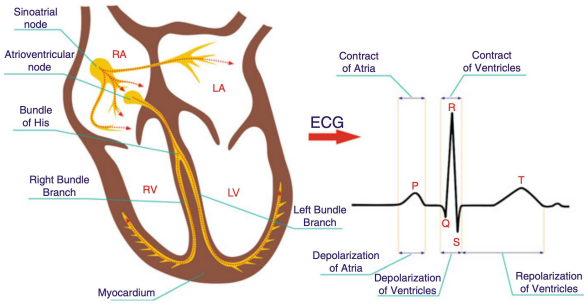

Fig. 1. Anatomy of the Human Heart alongside features of ECG Wave. RA stands for Right Atrium, LA stands for Left Atrium, RV stands for Right Ventricle, LV stands for Left Ventricle [4].

B. ECG Wave Characteristics

The ECG signal is representative of the electrical conduction of the heart. They has certain characteristic features (Fig. 1 Right) understanding which is necessary in order to process these signals. These characteristics are briefly described below [5].

1) P-Wave: The P-wave results from the depolarization of the atria. It usually is 0.12 s long and has a max amplitude of 0.15 mV. Most of the spectral content of the P-wave in the 10 Hz range. It is interesting to note that no atrial repolarization is seen as it is masked by the depolarization of the ventricles. The time elapsed between the end of a P-wave to the start of the Q-wave (known as PQ segment) signifies time gap between the depolarization of atria and ventricle. This segment is no more that 0.2 s.

2) QRS-Complex: The QRS-complex represents the ventricular depolarization. It is the largest wave group in the ECG, having an amplitude between 1.5 mV - 2.0 mV. The duration of the complex does not exceed 0.12 s. A heart beat, or more technically a cardiac cycle is the time elapsed between two consecutive R peaks. A notable proportion of the spectral content of the QRS-complex in the 40 Hz range.

This report was made as part of UCSB ECE 258: Multirate Digital Signal Processing Course Project

[1]singular: atrium

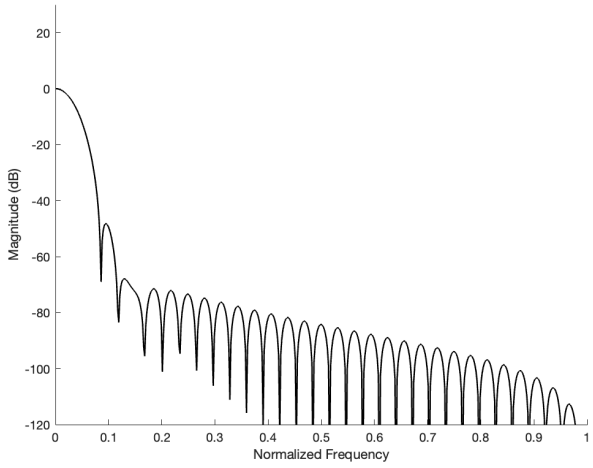

Fig. 2. Magnitude response of the Prototype Filter

3) T-Wave: The T-wave marks the end of the repolarization of the ventricles. In the interval between a T-wave and P-wave (known as the TP segment), the heart muscles relax and blood fills up in the heart. Like the P-wave, T-wave's spectral content extends upto 10 Hz.

III. Filter Bank Fundamentals

As described in the previous section, the various waves of the ECG signal have their energy content distributed in various frequencies. Hence, it is prudent to analyse the signal by breaking it into its constituent subbands. In this section, the fundamentals of filter bank design is described [6].

A. FIR Filter Design by Windowing

The windowing method is one of the simplest ways for constructing a FIR filter with desired frequency response.

As shown in [7], the design process begins with a desired frequency response $H_d(e^{jw})$. The desired impulse is then calculated as follows:

$$h_d(n) = \frac{1}{2\pi}\int_{-\pi}^{\pi} H_d(e^{jw})dw$$

From this a causal FIR filter with L taps can be defined as

$$h(n) = \begin{cases} h_d(n) & 0 \le n \le L \\ 0 & \text{otherwise} \end{cases}$$

More generally, the FIR filter can be viewed as a windowed version of the desired frequency response.

$$h(n) = h_d(n) * w(n)$$

It is clear to see that in the above example, $w(n)$ would be a rectangular window. In this report, the prototype filter, as shown in Fig. 2 was designed to have a cutoff of $\frac{\pi}{M}$ using a hamming window.

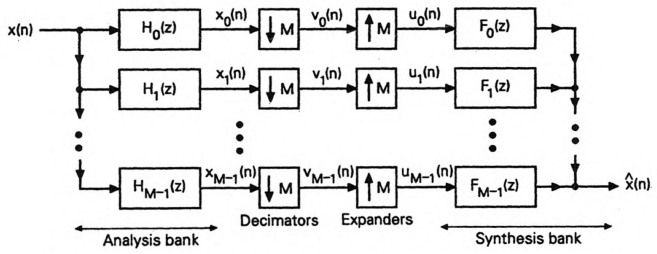

Fig. 3. M-Channel Filter Bank [6]

B. M-Channel Filter Bank Fundamentals

An M-channel filter bank is shown in Fig. 3. It contains M analysis and M sythesis filters, each with L-taps. Given a prototype lowpass filter $H_0(z)$, all the other $M-1$ filters i.e., $H_i(z),\ i = 1, \ldots, M-1$ are frequency shifted versions of the prototype, such that they span the entire bandwidth of the input signal. For the purpose of this project, the prototype filter was designed using the window method (see Appendix).

Using analysis the filters, $H_0(z), H_1(z), \cdots, H_{M-1}(z)$, the corresponding subbands are calculated as:

$$X_i(z) = H_i(z)X(z);\ i = 0, 1, \cdots, M-1 \tag{1}$$

Each of these subbands has a normalized bandwidth of $\frac{1}{M}$ which allows for the M^{th} order decimation of each of the subbands. The decimated output can be represented as follows:

$$V_i(z) = \frac{1}{M}\sum_{k=0}^{M-1} X_i(z^{\frac{1}{M}}W^k);\ i = 0, 1, \cdots, M-1 \tag{2}$$

where $W = W_M = e^{-j\frac{2\pi}{M}}$ is the twiddle factor. Note the $W_i(z)$ is a bandpassed and decimated version of the input signal $X(z)$. The decimation allows for the subband processing rate to be $1/M$ of the original signal rate which makes it computationally efficient. This is the concept of a polyphase representation and for more details please read [6].

When reconstructing the signal, $V_i(z)$ is first interpolated by an order M and then passed through the sythesis filters, $F_0(z), F_1(z), \cdots, F_{M-1}(z)$. The final reconstructed signal is

$$\hat{X}(z) = \frac{1}{M}\sum_{k=0}^{M-1} X(zW^k)\sum_{i=0}^{M-1} H_i(zW^k)F_i(z) \tag{3}$$

For ease of analysis, the above equation is rewritten as follows

$$\hat{X}(z) = \sum_{k=0}^{M-1} A_k(z)X(zW^k) \tag{4}$$

where

$$A_k(z) = \frac{1}{M}\sum_{i=0}^{M-1} H_i(zW^k)F_i(z) \tag{5}$$

C. Perfect Reconstruction

For $k > 0$, $X(zW^k)$ represents the shifted (or aliased) versions of $X(z)$ which distort the reconstructed signal $\hat{X}(z)$. These versions originate from the decimation and interpolation due to the non-idealities in the analysis and synthesis filter banks. In order to have a distortion free reconstruction signal, we require

$$A_k(z) = 0; \ k = 1, \cdots, M-1 \tag{6}$$

$$\implies \hat{X}(z) = A_0(z)X(z) \tag{7}$$

Such a filter bank where no distortion or aliasing effects are present is called a perfect reconstruction filter bank (PR FB). Consequently, in a PR FB, $A_0(z)$ is just a pure time delay and all the aliasing terms are zeroed out. The time domain reconstructed signal will

$$\hat{x}(n) = cx(n - n_0) \tag{8}$$

where c is some constant gain and n_0 is delay.

D. Linear Phase

In order to ensure that the signal experiences a pure time delay, all the filters in the PR FB should have linear phase. The reason for this is that frequency is the rate of change of phase. If the frequency response of a filter has linear phase, then the signal that passes through the filter experience a uniform shift in its phase which, in time domain, is seen as a constant delay. In case of FIR filters, linear phase is easily enforced by ensuring that the filter coefficient are real and symmetric. The proof for this is elementary and can be found in [7].

E. Paraunitary

Given a matrix $\mathbf{H}(z)$, if it satisfies

$$\tilde{\mathbf{H}}(z)\mathbf{H}(z) = \mathbf{I}$$

then $\mathbf{H}(z)$ is said to be paraunitary or lossless[2] [8]. This property is very useless as it simplifies the inverse of $\mathbf{H}(z)$ to

$$\mathbf{H}^{-1}(z) = \tilde{\mathbf{H}}(z)$$

and if analysis bank has only real coefficients, then

$$\mathbf{H}^{-1}(z) = \mathbf{H}^T(z)$$

F. Perfect Reconstruction FB Design

For this project a 32-channel PR FB was constructed using the method shown in [6], [8] and is briefly presented below for completion. The generated 32 analysis filters are shown in Fig. 4.

Equation (3) can be written in a matrix-vector form as follows

$$\hat{X}(z) = \frac{1}{M}\mathbf{f}^T(z)\mathbf{H}^T(z)\mathbf{X}(\mathbf{z}) \tag{9}$$

[2]Note that $\tilde{\mathbf{H}}(z)$ is the conjugate transpose of $\mathbf{H}(z)$

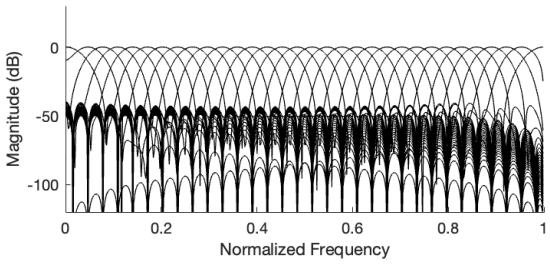

Fig. 4. Frequency Magnitude Response of 32 Analysis Filters.

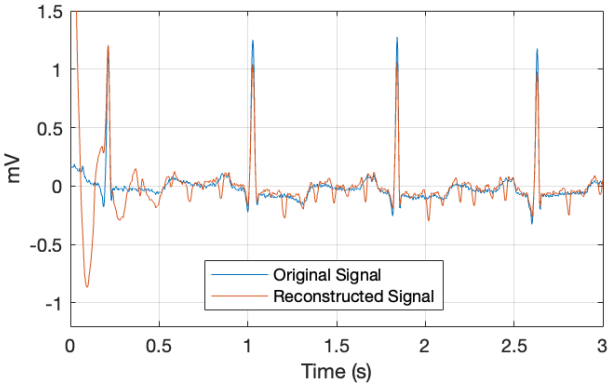

Fig. 5. The orginal signal and its reconstructed version.

where $\mathbf{f}(z) = [F_0(z), F_1(z), \cdots, F_{M-1}(z)]^T$ and $\mathbf{X}(z) = [X(z), X(zW^{-1}), \cdots, X(zW^{-(M-1)})]$. The matrix $\mathbf{H}(z)$ is called the Alias-Component matrix and is defined as:

$$\mathbf{H}(z) = \begin{bmatrix} H_0(z) & \dots & H_{M-1}(z) \\ H_0(zW^{-1}) & \dots & H_{M-1}(zW^{-1}) \\ \vdots & \ddots & \vdots \\ H_0(zW^{-(M-1)}) & \dots & H_{M-1}(zW^{-(M-1)}) \end{bmatrix}$$

from Equation (6), it is clear that

$$\mathbf{H}(z)\mathbf{f}(z) = [cz^{-n_0}, \ 0, \ \dots \ 0]^T \tag{10}$$

$$\implies \mathbf{f}(z) = \mathbf{H}^{-1}(z)[cz^{-n_0}, \ 0, \ \dots \ 0]^T \tag{11}$$

In the above equation, if we impose the paraunitary and linear phase constraints on $\mathbf{H}(z)$, then it can be shown that

$$F_i(z) = z^{-(L-1)}H_i(z^{-1})$$

which in time domain becomes

$$f_i(n) = h_i(L - 1 - n) = h_i(n)$$

Again, it is to be noted that the above analysis is highly concise and an in-depth treatment of the same is presented in [6], [8]. Fig. 5 shows the original and the reconstructed signal using the above mentioned method. For a more precise reconstruction, one can increase the number of taps in the filter bank.

Note that the PR FB was designed only as an academic exercise. ECG beat detection only requires the decomposition of the signal into its subbands and does not need any reconstruction [9].

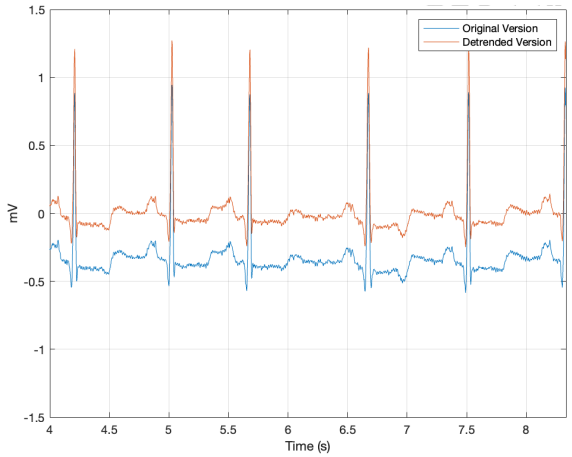

Fig. 6. Removal of Baseline Wander using Detrending. Blue is the original signal and red is the detrended version.

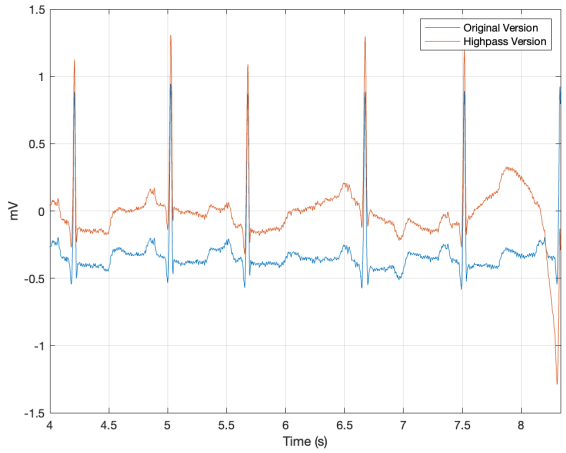

Fig. 7. Removal of Baseline Wander using Filtering. Blue is the original signal and red is the highpass version.

IV. Detecting the Beats

Based on the fundamentals provided in the previous sections, the pipeline for detecting beats from the subbands is now presented. More specifically, the detection of the QRS complex is shown. This detection logic is a slightly modified version of level 1 algorithm provided in [9].

A. Premilinary Observations

The signal used in this report is from the MIT/BIH arrhythmia dataset [10] and was obtained from PhysioNet [11]. The ECG signal is half an hour long; recorded at a rate of 360 Hz. Hence the total bandwidth of the signal is 180 Hz. The signal is not MATLAB compatible out of the box and was converted to MAT file format using python[3].

B. Baseline Wandering

Sometimes in the ECG signals, DC component of the signal is not constant and it "wanders" around, assuming a trend. This phenomenon is called baseline wandering. It occurs when the impedance between the body and electrode changes and it appears as a low frequency noise. Typically, this noise is below 1 Hz but there are cases where the baseline wandering can go upto a few hertz. In this report, two ways of suppressing this effect are considered. These are detrending (time-domain) and filtering (frequency-domain).

Detrending is the processing of constructing a polyline fit of the mean of the signal and later, removing this polyline from the signal, which zeroes out the trend of the mean or the DC component of the signal. Note that this process is performed on the time-domain signal directly. Detrending is shown in Fig. 6.

Filtering, as the name suggests, tries to filter out the frequencies responsible for baseline wandering. Typically, a highpass filter with a cutoff of < 1 Hz is applied onto the signal. Filtering is shown in Fig. 7.

There is a trade-off in accuracy and computation efficiency in the 2 methods. Detrending is more accurate but also computationally intensive as the entire signal has to be traversed inorder to create the polyline. Filtering is less accurate due to edge effects but it is computationally efficient, when compared to detrending.

[3]The conversion file is available at https://github.com/Kapi2910/heart-beat-258/blob/master/ecg.ipynb

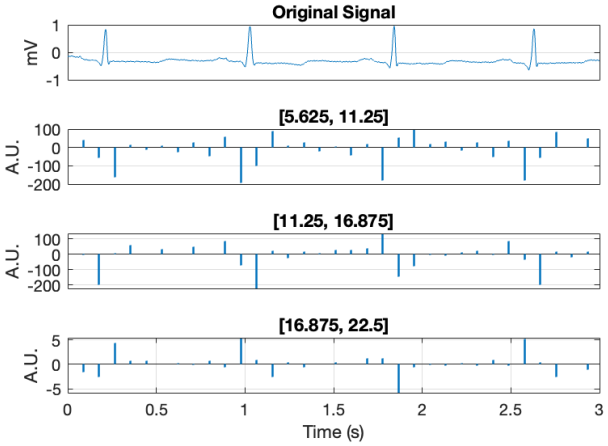

Fig. 8. Input ECG signal decomposed into subbands. Subbands corresponding to $[5.625,\ 11.25]$, $[11.25,\ 16.875]$, and $[16.875,\ 22.5]$,

C. Breaking into Subbands

The input signal is broken down into 32 uniform frequency subbands using the filter bank designed in Section III. This implies that the bandwdith of each subband is $\frac{180}{32} = 5.625$ Hz and the subbands themselves are $[0,\ 5.625]$, $[5.625,\ 11.25], \ldots,$ $[174.375,\ 180]$ some of which are illustrated in Fig. 8. The subbands are sampled at a rate of 11.25 Hz.

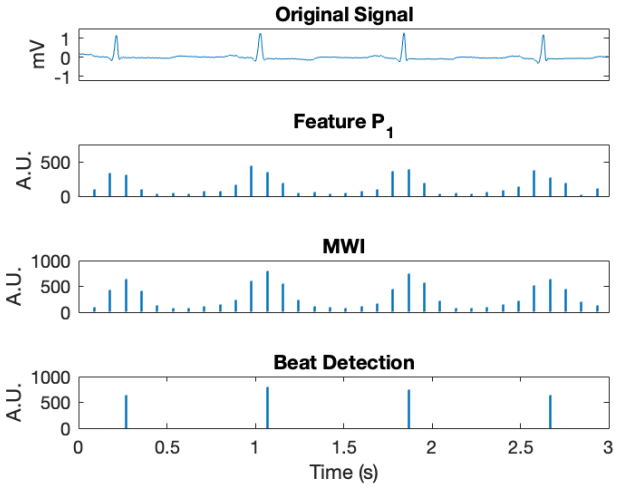

Fig. 9. Detecting the beats of the original signal using Feature P_1.

D. Feature Extraction

The features that mark the QRS complex can be formed by superposing subbands which are close [**?**] to the energy content of the complex. According [12], these are bands $V_1(z)$, $V_2(z)$, $V_3(z)$ and $V_4(z)$ which correspond to frequency ranges, $[5.625,\ 11.25]$, $[11.25,\ 16.875]$, $[16.875,\ 22.5]$ and $[22.5,\ 28.125]$. Feature P_1 was used to find the beat, which is calculated as follows:

$$P_1 = \sum_{i=1}^{3} |V_i(z)| \tag{12}$$

E. Detection Logic

The feature is sent through a moving window integrator (MWI). The peaks of the output of the MWI are the beats of the ECG signal. In the past [12], peaks were detected as the inflexion points i.e. the points where the second derivative is zero and no thresholding was performed. This method of detecting beats was used as first step in a more intricate process that accounts for the signal and noise histories [9]. In this project, peaks are detected using a heuristic threshold. Fig. 9 illustrates the entire beat detection logic. As can be clearly seen, there is a detection that corresponds to the positive peak of the QRS complex (R-wave).

V. Conclusion

The concepts presented in this report are well founded in the literature with robustness and explainability built into the pipeline. The project begins by presenting elementary ECG signal processing. Particularly, the origin and features of the ECG signal were explored thereby defining the heart beat as a signal characteristic. The spectral features of the various parts of the signal were also studied which necessitated the decomposition of the signal into various frequency subbands. To this end, a 32-channel filter bank was designed and used to calculate the feature that is derived from the subbands 1-3. This feature was further processed using MWI and a threshold was applied to finally detect the beats. Although perfect reconstruction is not a requirement for beat detection, the filter bank designed in this project can be utilised for other tasks such as ECG beat classification.

A. Modern ECG Signal Processing

With the advent of wearable health monitors, ECG signals and their analysis have become a core component of a healthy lifestyle. Hence, there is still a push towards more computationally efficient ways to process this signal due to the limited battery size of a wearable, such as a smartwatch. Additionally, research in machine learning and deep learning further elevates the potential of ECG analysis, enabling faster and more precise diagnoses [3]. It was very interesting to see that even in 2024, filter bank design with applications towards ECG signals are discussed [13].

References

[1] World Health Organization (WHO), "Cardiovascular diseases (CVDs)," 2021. https://www.who.int/news-room/fact-sheets/detail/cardiovascular-diseases-(cvds) (accessed December 02, 2024).

[2] J. Hoffmann, S. Mahmood, P. S. Fogou, N. George, S. Raha, S. Safi, K. J. Schmailzl, M. Brandalero, and M. Hübner, "A Survey on Machine Learning Approaches to ECG Processing," in *2020 Signal Processing: Algorithms, Architectures, Arrangements, and Applications (SPA)*, pp. 36–41, IEEE, 2020.

[3] W. Ahmed and S. Khalid, "Ecg signal processing for recognition of cardiovascular diseases: A survey," in *2016 Sixth International Conference on Innovative Computing Technology (INTECH)*, pp. 677–682, IEEE, 2016.

[4] A. Gacek, "An Introduction to ECG Signal Processing and Analysis," in *ECG Signal Processing, Classification and Interpretation: A Comprehensive Framework of Computational Intelligence*, pp. 21–46, Springer, 2011.

[5] J. Wasilewski and L. Poloński, "An Introduction to ECG interpretation," in *ECG signal processing, classification and interpretation: a comprehensive framework of computational intelligence*, pp. 1–20, Springer, 2011.

[6] P. P. Vaidyanathan, *Multirate Systems and Filter Banks*. Prentice Hall, Aug. 2023.

[7] A. V. Oppenheim, R. W. Schafer, and J. R. Buck, *Discrete-time signal processing*. Prentice Hall signal processing series, Upper Saddle River, N.J: Prentice Hall, 2nd ed. ed., 1999.

[8] H. S. Malvar, *Signal processing with lapped transforms*. The Artech House telecommunications library, Boston: Artech House, 1992.

[9] V. X. Afonso, W. J. Tompkins, T. Q. Nguyen, and S. Luo, "Ecg beat detection using filter banks," *IEEE transactions on biomedical engineering*, vol. 46, no. 2, pp. 192–202, 1999.

[10] L. Maršánová, A. Němcová, R. Smíšek, T. Goldmann, M. Vítek, and L. Smital, "Automatic detection of p wave in ecg during ventricular extrasystoles," in *World Congress on Medical Physics and Biomedical Engineering 2018: June 3-8, 2018, Prague, Czech Republic (Vol. 2)*, pp. 381–385, Springer, 2018.

[11] A. L. Goldberger, L. A. N. Amaral, L. Glass, J. M. Hausdorff, P. C. Ivanov, R. G. Mark, J. E. Mietus, G. B. Moody, C.-K. Peng, and H. E. Stanley, "PhysioBank, PhysioToolkit, and PhysioNet: Components of a new research resource for complex physiologic signals," *Circulation*, vol. 101, no. 23, pp. e215–e220, 2000 (June 13). Available at https://physionet.org/content/pwave/1.0.0/ (accessed November 15, 2024).

[12] V. X. Afonso, W. J. Tompkins, T. Q. Nguyen, and S. Luo, "Filter bank-based ECG beat detection," in *Proceedings of 18th Annual International Conference of the IEEE Engineering in Medicine and Biology Society*, vol. 3, pp. 1037–1038, IEEE, 1996.

[13] B. Keerthana, N. Raju, C. Ravikumar, R. Anbazhagan, T.-h. Kim, and F. Mohammad, "Designing optimal prototype filters for maximally decimated cosine modulated filter banks with rapid convergence," *Heliyon*, 2024.